Systematic study of the correlation between surface chemistry, conductivity and electrocatalytic properties of graphene oxide nanosheets

Giulio Maccaferri,[a,b] Chiara Zanardi,[a,*] Zhen Yuan Xia,[b] Alessandro Kovtun,[b] Andrea Liscio,[b,c] Fabio Terzi,[a] Vincenzo Palermo,[b,*] Renato Seeber[a,b]

[a] Department of Chemical and Geological Sciences, Università di Modena e Reggio Emilia, Via G. Campi 103, 41125 Modena, Italia.

[b] Istituto di Sintesi organica e Fotoreattività (ISOF), Consiglio Nazionale della Ricerca (CNR), via Gobetti 101 - 40129 Bologna, Italia.

[c] Istituto dei Sistemi Complessi (ISC), Consiglio Nazionale della Ricerca (CNR), via del Fosso del Cavaliere 100 - 00133 Roma, Italia.

Abstract

A main advantage of graphene oxide (GO) over other materials is the high tunability of its surface functional groups and of its electric conductivity. However, the complex chemical composition of GO renders difficult to unravel the correlation between structural and electric properties. Here, we use a combination of electron spectroscopy and electrochemistry to correlate the surface chemistry of GO to its electrical conductivity and electrocatalytic properties with respect to two molecules of high biological interest: β-nicotinamide adenine dinucleotide (NADH) and vitamin C. We demonstrate that the electrocatalytic properties of the material are due to hydroxyl, carbonyl and carboxyl groups residues that, even if already present on pristine GO, become electroactive only upon GO reduction.

The results of this study demonstrate the advantages in the use of GO in amperometric biosensing and in enzymatic biofuel cells: it allows the oxidation of the target molecules at low potential values, with a sensitivity >15 times higher with respect to standard, carbon-based electrode materials. Finally, we demonstrate that the right amount of chemical groups to achieve such high performance can be obtained also by direct electrochemical exfoliation of bulk graphite, without passing through GO production, thus rendering this approach suitable for cheap, large-scale applications.

*corresponding authors
Tel.: +39 059 205 8650. E-mail: chiara.zanardi@unimore.it (Chiara Zanardi)
Tel. +39 051 639 9824. E-mail: vincenzo.palermo@isof.cnr.it (Vincenzo Palermo)

1. Introduction

Graphene is one of the materials most studied nowadays for its numerous potential applications, including energy storage and sensing [1-5]. Outstanding performance of this nanosized material comes from its peculiar physico-chemical properties, such as high surface area (>2600 m^2/g for single-layer graphene), excellent thermal and electric conductivity and high mechanical strength.

Large-scale production methods of graphene are currently used also at industrial level [6]. However, they usually yield a mixture of graphene multilayers, with a variable amount of monolayers. The only method to achieve quantitative exfoliation of graphite down to single layers is by chemical oxidation, which yields graphene oxide (GO) solutions mostly composed of monolayers of carbon nanosheets [7,8]. The stability of GO suspensions is due to the high number of oxidized residues on the carbon surface; they favour the stability of GO in different solvents, water included, but render the material poorly conductive [9,10]. Due to its highly defective nature, GO has long been the underdog of the graphene family. However, this prejudice is now being challenged and GO is used for many interesting potential applications.

GO can be reduced by thermal, chemical and electrochemical procedures, in order to partially remove the oxidized functional groups and to re-establish sp^2 structure of the material. The material obtained is generally referred to as 'reduced graphene oxide' (RGO). Among the different methods used to such a purpose, the electrochemical approach allows fine tuning of the reduction level of the material, finally conditioning the surface chemistry and degree of interaction between adjacent graphene foils [11-13]. Correspondingly, the electrical conductivity of GO may be tuned from insulating to highly conductive [8,14], and the surface chemistry from highly hydrophilic to hydrophobic character [15]. Electrochemical methods can be also used for controlled functionalization of graphene nanosheets [16] as well for production of graphene-based electrodes [16] or of composite foams [17]. In recent years, electrochemical procedures have also demonstrated to constitute suitable tools for mass production of graphene from graphite [7,18] at industrial level.

Although it is well established that the elimination of oxidized functionalities improves the conductivity of the material [11], it was recently found that the residual oxidized groups, not removed by the reducing process, play a key role in the electrocatalytic properties of GO, as an example in favouring the electrochemical oxidation of gallic acid [13]. Electrochemical techniques are thus ideal to study both conductivity and electrocatalytic performance of GO at different degrees of reduction.

Even if several published works tried to study in detail the actual role played by the different functional groups on carbon nanosheets in the electrocatalytic performance of graphene, a clear explanation is still missing. The scenario is complicated by the lack of a definition of the chemical structure of the specific graphene used in many papers and by the possible presence of residual heavy

metal ions coming from the synthetic procedure, that can themselves induce electrocatalytic processes [19].

In this work we deposited GO nanosheets on commercial screen-printed electrodes (SPE), typically used for electrochemistry. The GO was then reduced to various degrees by applying an electrochemical potential, in order to study the role of the different oxygen functional groups present on the nanosheets in the electrocatalytic properties of the material, at the basis of the actual application of the material. For such a purpose, two particular chemical species of biological interest were used as the benchmarks: nicotinamide adenine dinucleotide (NADH) and ascorbic acid (AA), also known as vitamin C. As such, they constitute quite interesting benchmarks to test the electrocatalytic performance of the material, due to overvoltages affecting their electrochemical oxidation at bare surfaces [20, 21]. From an applicative point of view, they constitute two important chemical species that require to be detected in many biological frames by rapid and simple analytical systems. In particular, AA is one of the most important vitamins present in many biological and food matrices, whereas NADH/NAD^+ redox couple constitutes the cofactor of many oxido-reductase enzymes. The possible occurrence of electrocatalytic process in charge of this latter species may lead to quite efficient amperometric biosensors for a wide number of chemical species constituting the substrate of a defined enzyme [20] and to enzymatic biofuel cells [22-24].

GO films have been used as such or after *in situ* electrochemical pre-treatment at fixed negative potentials. Such a pre-treatment leads to formation of RGO films with increasing electrical conductivity, related to a decreasing number of hydrophilic oxygen groups on its surface. The electrochemical and electrocatalytic performance of graphene films was correlated to the functional groups present at the material surface, measured by X-ray photoelectron spectroscopy (XPS). To understand the effect of oxygen-based functional groups on the performance of graphene, we also chemically modified the graphite electrode surface by electrochemical oxidation/activation of the surface [25] and subsequent deposition of hydroquinone (HQ) and catechol (CT) molecules.

The tunable electrochemical reduction of GO allows the obtainment of the right amount of defects to foster the electrocatalytic oxidation of both NADH and AA at low potential values.

The right surface chemistry and the good electrocatalytic performance can be achieved also skipping completely GO preparation-reduction steps, by direct use of electrochemically exfoliated graphene oxide (EGO). This material, directly obtained by electrochemical oxidation and exfoliation of bulk graphite, is more suitable than GO for large scale industrial applications because it can be obtained at low cost and high speed, without using the harsh chemical or solvents necessary for the production of GO or of graphene [7, 16, 17, 26].

2. Experimental Section

2.1 *Chemicals*

All reagents were of analytical grade and supplied by Sigma-Aldrich.

GO was prepared from graphite flakes (Sigma Aldrich, 99% pure, < 150 μm) using a modified Hummer's method, as described in Ref. [27]. The GO water suspension produced was then subjected to dialysis to remove residual metal ions and acids. The amount of residual Mn, which is the most abundant metal introduced in the synthetic process, resulted lower than 2.7 ppm, as determined by Inductively Coupled Plasma Mass Spectrometry (ICP-MS, XSeries II Thermo Fisher Scientific). The purified GO dispersion was sonicated for about 1.5 h, and unexfoliated GO was removed by centrifugation (3000 rpm, 5 min). The concentration of the resulting GO aqueous suspension was 4.0 gL^{-1}.

A stable suspension of EGO in DMF was prepared from graphite flakes (Sigma Aldrich, 99% pure, < 150 μm) according to the method previously reported in Ref. [26]; the use of the same commercial graphite stock for EGO and GO production allows a correct comparison between the performance of the different materials. Due to the low stability of SPEs in DMF, EGO was transferred into an isopropyl alcohol (IPA) solution.

In order to allow a direct comparison between EGO and GO modified electrodes, both materials were deposited on the electrodes from a 0.5 gL^{-1} solution in IPA with a loading of 0.020±0.002 mg cm^{-2}.

2.2 *Instruments*

All electrochemical measurements were performed using a computerized Autolab PGSTAT 30 (Ecochemie, Utrecht, The Netherlands). SPEs were acquired from DropSens (Llanera, Asturias, Spain) and consisted of a 4 mm diameter graphite working electrode, a graphite auxiliary electrode and an Ag pseudo-reference electrode.

The XPS measurements were performed on each deposit with a Phoibos 100 hemispherical energy analyser (Specs), using Mg Kα excitation source (XR-50, Specs) (photon energy = 1253.6 eV). The X-ray power was 250 W. The base pressure in the analysis chamber during analysis was 2×10^{-10} mbar.

The morphology of the working electrode surfaces was investigated by a Nova NanoSEM 450 scanning electron microscope (SEM, FEI Company) working in high vacuum conditions, equipped with an Energy Dispersive Spectrometer (EDS, Bruker QUANTAX-200).

Raman spectra of modified electrode surfaces have been registered with a Laser DXR (532 nm laser wavelength at 1 mW laser power).

Change in work function among the different electrode coatings was measured using two experimental techniques such as macroscopic Kelvin Probe (KP) and Kelvin Probe Force Microscopy (KPFM) performed under ambient conditions.

Macroscopic KP measurements were performed using 2 mm diameter gold tip amplifier (Ambient Kelvin Probe Package KP020 from KP Technology Ltd, UK). The technique provides a voltage resolution of about 5 mV. Calibration of the probe was performed comparing two reference surfaces: aged gold thin film evaporated on mica and freshly cleaved High Oriented Pyrolytic Graphite. A comprehensive description of the technique can be found in Baikie et al.[Baikie et al., Method. Rev. Sci. Instrum. 1991, 62, 1326−1332].

KPFM measurements were performed by employing a commercial microscope Multimode 3 (Bruker) with Extender Electronics module. In order to obtain a sufficiently large and detectable mechanical deflection, we used ($k = 2.8\ N{\cdot}m^{-1}$) Pt/Ir coated Si ultra-levers (SCM-PIT, Bruker) with oscillating frequencies in the range $60 < u < 90$ kHz. AFM and KPFM images were acquired in the same measurement; a topographic line scan is first obtained by AFM operating in tapping mode and then that same line is rescanned in lift mode with the tip raised to a lift height of 100 nm. KPFM technique provides a voltage resolution of about 5 mV and a lateral resolution of a few tens of nanometers. Comprehensive description of the two techniques can be found in [Liscio et al., Acc. Chem. Res., 2010, 43, 541–550 and Musumeci et al., Mat Today, 2014, 17, 504–517] and references therein.

2.3 *Preparation of modified electrodes*

GO/SPEs were prepared by drop casting 4 μL of 0.5 gL^{-1} GO suspension in IPA onto the SPE working electrode. The solvent was allowed to evaporate at room temperature. The amount of GO finally present on each electrode was 0.020±0.002 mg cm^{-2}, corresponding to an average thickness of about 110 nm, assuming a GO density of 1.8 g cm^{-3} [28].

RGO/SPEs, consisting of GO coatings at different reduction degree, were obtained by pre-treating the electrodes at controlled potential ($E_{pre\text{-}treat}$). The potential was applied for 300 s in a 0.1 M phosphate buffer solution, pH 7.0 (PBS). Five groups of samples were obtained, named $RGO_{\text{-}0.25V}$, $RGO_{\text{-}0.50V}$, $RGO_{\text{-}0.75V}$, $RGO_{\text{-}1.00V}$, and $RGO_{\text{-}1.25V}$, where the subscript indicates the potential used for the pre-treatment.

Activated SPEs (SPE_{Act}) were obtained by performing 10 subsequent voltammetric cycles between -1.0 and +1.7 V, at 0.1 Vs^{-1} potential scan rate, in 1 M H_2SO_4 solution [25]. Deposition of HQ and CT onto SPE_{Act} was achieved by performing ten subsequent potential scans from +0.8 to −0.1 V, at 0.02 Vs^{-1} potential scan rate, in a 1 mM HQ and 1 mM CT, 0.1 M acetate buffer solution

(pH 4.0), respectively [25]. The resulting electrode (HC/SPE) was thoroughly rinsed before any electrochemical tests.

EGO/SPEs were prepared by dropping 0.5 gL^{-1} EGO dispersion in IPA onto the working electrode of SPEs. The solvent was allowed to evaporate at room temperature. The amount of EGO finally present on each electrode was 0.020±0.002 mg cm^{-2}. All EGO/SPEs were used directly without any electrochemical pre-treatment.

2.4 *Electrochemical measurements*

Linear sweep voltammetry (LSV) and cyclic voltammetry (CV) were chosen as the electrochemical techniques to correlate the electrochemical and electrocatalytic properties of GO, RGO and EGO films to the chemical nature of functional groups at the electrode|solution interface, as defined by XPS and Raman measurements. In order to investigate the characteristics of the charge percolation through the coating and of the transfer process at the different modified electrodes, CV traces were recorded in 5 mM $[Fe(CN)_6]^{3-/4-}$, 0.1 M $LiClO_4$, aqueous solution, in the -0.30 to +0.55 V potential interval, at 0.05 Vs^{-1} potential scan rate. Electrochemical Impedance Spectroscopy (EIS) tests have been also performed in the same solution, in order to confirm the results of the CV tests; to this aim, the electrode was polarised at the open circuit potential and an *ac* perturbation of 5 mV amplitude, in the 0.05 ÷ 10000 Hz frequency range, was applied.

The electrocatalytic performance of modified SPEs was tested in 0.1 M PBS (pH 7.0) containing either 0.2 mM NADH or 4 mM AA, by recording subsequent CV curves in the -0.2 to +0.7 V potential range, at 0.020 Vs^{-1} potential scan rate. 0.1 M KCl was added to all solutions used for electrochemical tests, in order to refer all potentials reported here to the $Ag|AgCl|Cl^-$ half-cell.

Differences in the electrocatalytic properties of the different materials were estimated from the mean values of the peak potentials and the associated standard deviations, measured for each material on at least three SPEs realized under the same conditions.

Calibration curves for NADH oxidation were obtained from measurements on bare and EGO modified SPEs, in solutions at minimum concentration of 30 μM. The calibrations were made plotting the steady state currents registered at +0.20 V fixed potential, under continuous stirring.

2.5 *X-ray photoelectron spectroscopy*

XPS spectra were recorded in the constant analyzer energy (CAE) mode with analyzer pass energies of 40 eV for the survey spectra and 20 eV for the high resolution ones, with an overall energy resolution of 1 eV determined on Ar^+ sputtered Ag ($3d_{5/2}$). The lens was set in high magnification

mode in order to achieve a 1 mm diameter spot area on the sample. Charging effects were corrected by energy calibration on C 1s level relative to 284.4 eV. High-resolution XPS spectra of C 1s were analyzed by CasaXPS (Casa software, Ltd), realising a nonlinear least-squares fitting procedure. The curve fitting was carried out using an asymmetric peak (i.e. Doniach-Sunjic line shape) [29] for the C=C bond (FWHM 1.2 eV), previously measured on the C 1s asymmetric peak of freshly cleaved and oxygen-free HOPG (grade ZYH, Advance Ceramics, US) [30]. The shifted components were modelled with symmetric Gaussian/Lorentzian curves shape with a full width half-maximum (FWHM) of about 1.4 eV [10].

3. Results and Discussion

3.1 *XPS, SEM and Raman characterization of GO and RGO*

XPS analysis allowed us to monitor the changes in oxidation degree and surface chemistry of GO upon electrochemical reduction at different potentials. XPS analysis unambiguously identifies the chemical nature and amount of the different functional groups present on the surface of the electrode.

GO surface chemistry and oxidation degree depend strongly on the production method. Since the GO used in the present article is different from that reported in similar studies present in the literature [11], measurements were performed on both pristine GO and RGO coatings used here. Fig. 1 reports the XPS spectra of SPEs modified by GO and RGO obtained at different applied potentials, namely $RGO_{-0.75V}$, $RGO_{-1.00V}$, and $RGO_{-1.25V}$. The spectrum of the bare, graphite-based, SPE surface is also reported for comparison. The XPS spectrum acquired on the sample treated at -0.50 V is reported in Supporting Information section (Fig. S1).

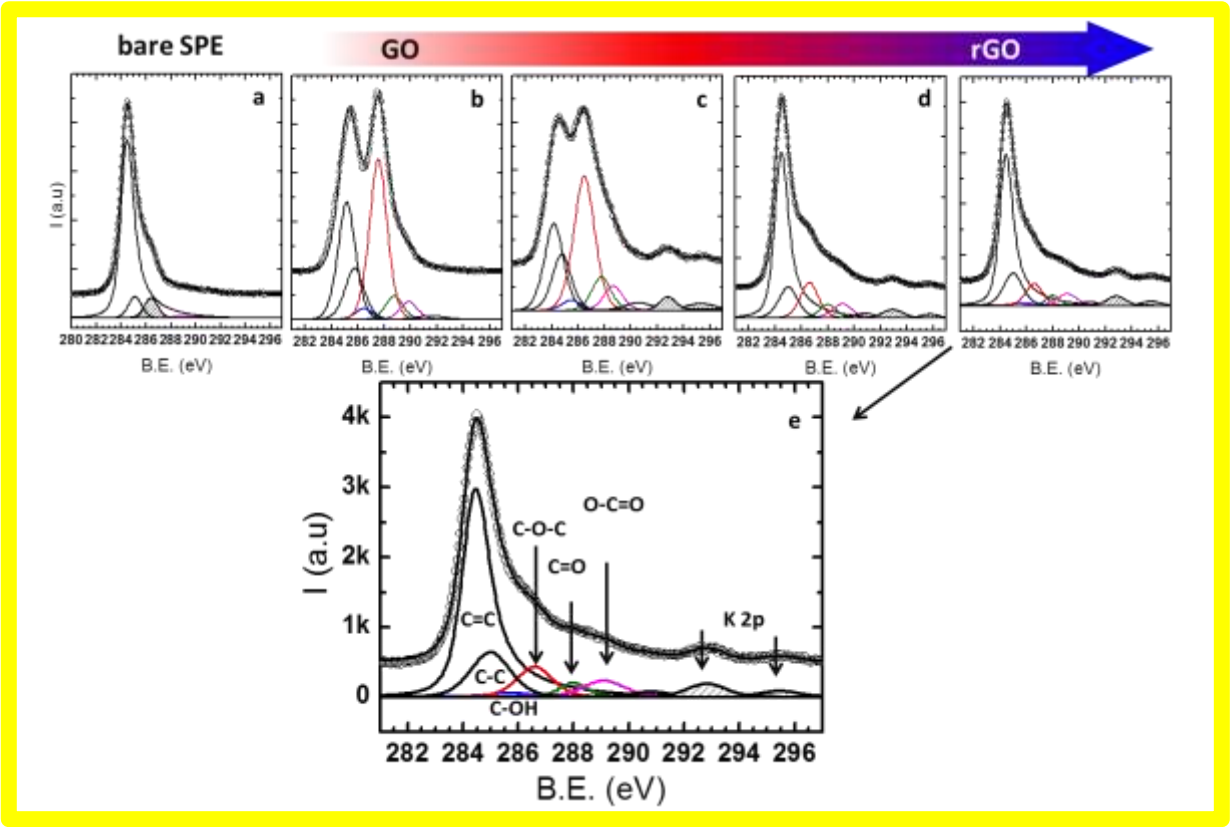

Fig. 1. High resolution XPS spectra of *(a)* bare SPE and SPE coated with *(b)* GO, *(c)* $RGO_{-0.75V}$, *(d)* $RGO_{-1.00V}$, *(e)* $RGO_{-1.25V}$. This last spectrum is shown also in large scale, to better evidence the different peaks contributing to the signal. The peaks at ca. 293 and 295 eV are due to potassium ions present on the substrate.

XPS spectrum of bare SPE (Fig. 1a) shows that: *i)* a very low amount of oxygen is bonded to the carbon atoms; *ii)* the C 1s peak has the typical graphitic asymmetric shape due to spectral features ascribable to C-OH and O-C=O residues localized at edge-vertex defects; *iii)* a characteristic peak is present in the Cl 2p region (Cl $2p_{3/2}$ at 200.0 eV, not shown), ascribable to a binder polymer used for electrode printing process. The analysis is in agreement with the technical specification of the SPE electrode.

After GO deposition, the GO/SPE surface presents the typical XPS spectrum of bulk, pristine GO (reported in Fig. S2 in Supporting Information). All samples show similar features in the high resolution spectra collected in the region of C 1s: a main graphitic peak at 284.4 eV and further peaks with lower intensity ascribable to C-C (shifted +0.7 eV in energy respect to the position of the main peak), C-OH (+1.5 eV), C-O-C (+2.3 eV), C=O (+3.6 eV) and O-C=O (+4.7 eV) moieties [9,10]. All

the C 1s spectra also present the expected peak due π-π* transition, located at +6.4 eV with respect to the main peak.

In all GO coated samples the peak in the Cl 2p region, characteristic of the bare SPE, is absent, suggesting that GO forms a uniform coating on the whole electrode, with a film thickness larger than the escape depth of the photoelectrons emitted from the film (≈10 nm with our setup). The uniformity of the film is confirmed by SEM measurements performed on the electrodes after coating (Fig. 2*b*). In particular, a flat morphology is observed, with ripples and folds typical of 2-dimensional materials, significantly different from the morphology of the uncoated SPE (Fig. 2*a*).

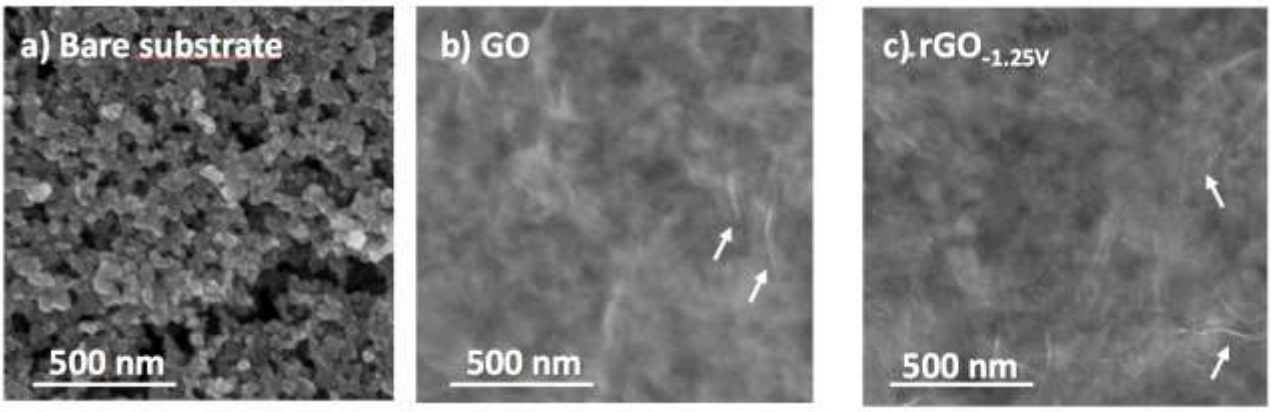

Fig. 2. FEG-SEM images collected by secondary electrons at *(a)* bare SPE, *(b)* GO/SPE and *(c)* RGO-$_{1.25V}$/SPE. White arrows indicate ripples typical of 2-dimensional nanosheets.

The C/O ratio of all samples was calculated by XPS data, in accordance with the stoichiometry of the previously described chemical groups fitted in the C 1s region. The alternative method, consisting in calculating the ratio between the C 1s and the O 1s peaks, was discarded because it overestimates the amount of oxygen, due to water molecules adsorbed on the surface. For applied bias down to -0.75 V, C/O ratio does not change significantly (Fig. 3*a*). A significant change is instead detectable after a pre-treatment at potentials lower than -0.75 V. Reduction of GO at potential values lower than -1.25 V was not possible, due to the massive evolution of H_2, leading to irreversible damage of GO films and to exposition of the underlying SPE electrode surface to the electrolyte solution.

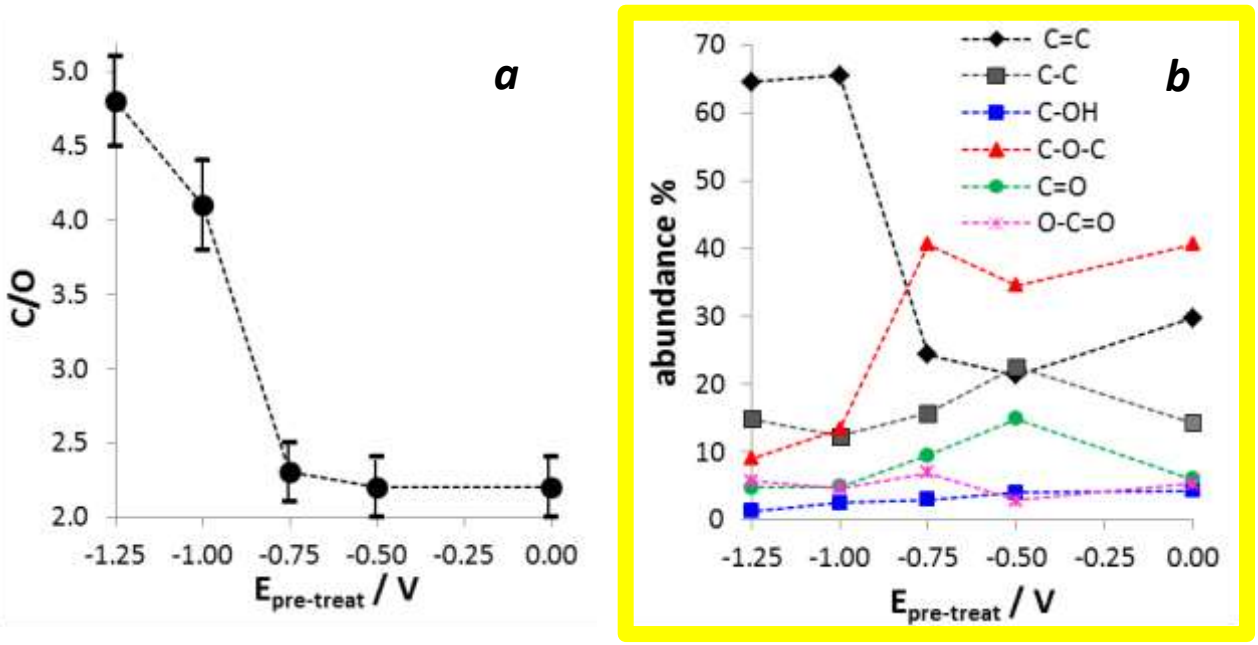

Fig. 3. *(a)* C/O ratio and (*b)* abundance percentage of different functional groups, as a function of the negative potential value applied in the electrochemical pre-treatment, calculated on the basis of XPS spectra of GO and RGO modified electrodes.

XPS allowed us also to measure the abundance of different functional groups on the sample surface (Fig. 3*b*). Precise abundance values, also measured on pristine SPE for comparison, are available in Table S1 in SI. The most significant effect of the electrochemical pre-treatment was a strong decrease of the number of epoxy groups, in agreement with results previously published in literature [11]. As expected, the disappearance of C-O-C functionalities occurs concurrently to the increase of peaks associated to C=C carbon moieties, suggesting the actual restoration of the aromatic structure of graphitic rings. On the contrary, the amount of C=O, C-OH, O-C=O and C-C groups is not significantly affected by the reduction process, operating within the potential interval considered. The application of more negative potentials is necessary to remove these oxidised moieties, as also suggested in ref. [11]. The amount of oxygen-containing functional groups is, anyway, significantly higher on GO modified SPEs than on pristine, graphite based, electrode surface (see Table 1 in Supporting Information).

To confirm the crystal structure, disorders and defects changes on GO surface induced by the electrochemical reduction, we also performed Raman spectroscopy measurements on GO and RGO-$_{1.25V}$ modified SPEs (see Fig. S3 in Supporting Information). As expected, the Raman spectrum of GO shows two main peaks: the disorder induced peak at 1353 cm^{-1} (D peak) and the E_{2g} phonon graphitic peak at 1600 cm^{-1} (G peak). After electrochemical reduction, the position of G peak (1599

cm^{-1}) remains almost unvaried, while the D peak results slightly downshifted to 1345 cm^{-1}. Concurrently, the I_D/I_G peak intensity ratio increases from 1.03±0.01 (GO) to 1.22±0.01 ($RGO_{-1.25}$), as a consequence of the reduction process. These results are consistent with literature reports concerning the effects of either chemical or electrochemical reduction treatments [31-33], confirming that the electrochemical reduction performed by us removes oxygenated functional groups (especially the epoxy group), and increases the average size of the sp^2 domains.

3.2 *Study of the charge transfer resistance of GO and RGO*

The resistance to charge percolation and transfer at the interface with the solution was estimated, for both GO and RGO films, from CV curves relative to anodic oxidation, and associated cathodic reduction, of a reversible redox couple, namely $[Fe(CN)_6]^{3-/4-}$ (see Fig. S4 in Supporting Information). In particular, the difference between anodic and cathodic peak potentials (ΔE) gives a measure of the conductivity of the electrode coating, assuming a value close to 60 mV for the redox system chosen when the resistance of the electrode is negligible. As expected [11], the ΔE value significantly decreases passing from GO to $RGO_{-1.25V}$ (Fig. 4*a*). The trend observed for coatings with increasing reduction degree (Fig. 4*b*) indicates that the reduction at potentials lower than -0.75 V renders the GO coating more and more conductive. The observed differences are reliable, resulting significantly larger than the standard deviation associated to each set of ΔE values, calculated on curves registered for three different SPEs. We could observe that the resistance of the film reaches a minimum by application of a potential of -1.0 V. Furthermore, consecutive CV curves registered on the same coating are well overlapped to each other, indicating that the modification of the GO coating due to electrochemical pre-treatment is stable.

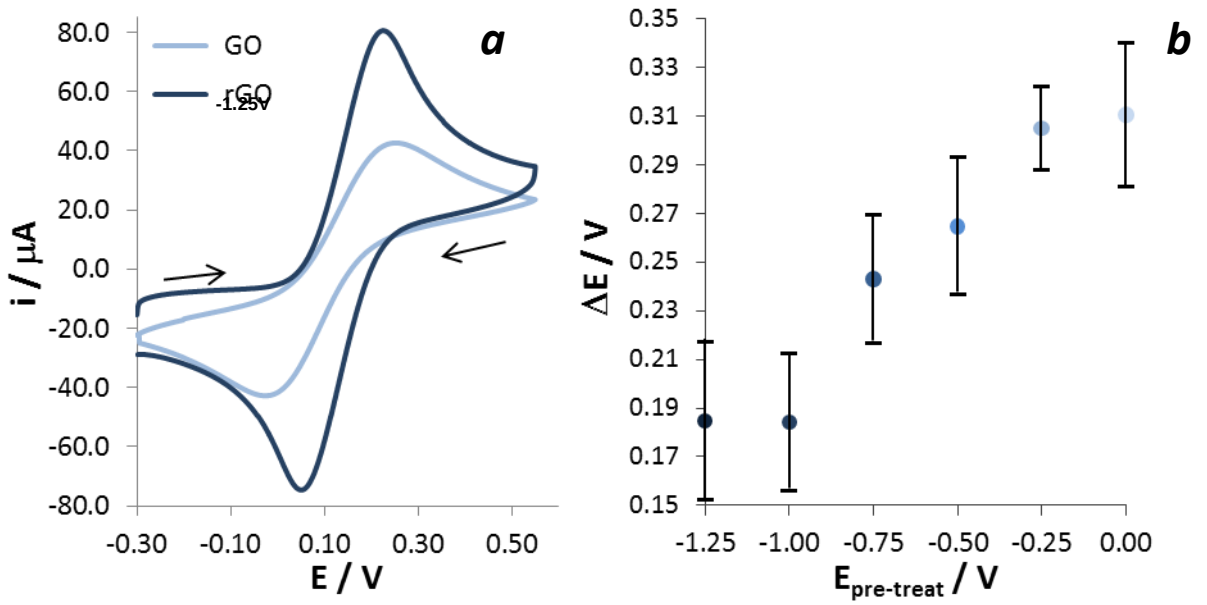

Fig. 4. *(a)* Representative CV curves (0.05 Vs^{-1} potential scan rate) recorded at GO and $RGO_{-1.25V}$ modified SPEs in aqueous solution containing 5 mM $[Fe(CN)_6]^{3-/4-}$, 0.1 M in $LiClO_4$, and 0.1 M KCl; (*b)* mean values and relevant standard deviations of ΔE registered on three graphene modified SPEs obtained at GO and RGO coatings at different reduction degree, under the same experimental conditions. The ratio between cathodic and anodic peak current, computed according to the semi-empirical formula reported in Ref [34], is always quite close to 1.

EIS plots collected at different graphene coatings in the same $[Fe(CN)_6]^{3-/4-}$ solution (see Fig. S5 in Supporting Information) support the conclusion carried out from CV experiments: by simulating the EIS spectra with a simple Randles circuit [36], the resistance of the system to charge transfer (R_{CT}) decreases at increasing the negative potential applied in the electrochemical pre-treatment.

The trend observed for the resistance can be explained on the basis of XPS and Raman results, which show a significant increase of sp^2-hybridized areas present on the sheets [8-10].

Fig. 4*a* shows that the height of the oxidation and reduction peaks (i.e. the charge passing across the material and at the material|solution interface) increases by passing from GO to $RGO_{-1.25V}$. This behaviour can be explained only in part assuming a higher reversibility degree of the system [35] directly connected to higher conductivity of the electrode coating. On the other hand, SEM images collected at GO (Fig. 2*b*) and $RGO_{-1.25V}$ films (Fig. 2*c*) rule out any evident changes in the morphology of the film. This indicates that the high current values registered can not be ascribed to an increase of the roughness of the coating, affecting the geometric surface area or the possible arising of radial diffusive regimes induced by the nanostructured surface [35,37]. As a consequence, the current increase should be accounted for by an increase of the electrochemically active area: the

increased conductivity of the film, both within each sheet and among different sheets, allows a wider fraction of the nanostructured surface to be electroactive with respect to the $[Fe(CN)_6]^{3-/4-}$ redox system. Furthermore, only when the material is well conductive, the nanosized morphology of the coating can also induce efficient regimes of radial diffusion [35,37] which can be also taken into account to explain the even higher currents registered at $RGO_{-1.25V}$ modified electrodes.

Finally, as expected, the conductivity decreases at increasing the thickness of the coating: thicker GO films (not shown) possess higher resistance and, upon reduction, exhibit larger decrease in ΔE values, thus larger increase in conductivity.

3.3 Study of the electronic properties in GO and $RGO_{-1.25V}$ coatings

Doping, vacancies and as well as oxygen functional groups affect the electronic structure of graphene-based materials, such as the density of state (DOS) and the corresponding electrical properties. In addition to the variation of the electrical resistance, the change of DOS leads to the tuning of a so-called quantum capacitance term, that significantly alter the electrochemical behaviour of graphene. (see refs [Adv. Mater. 2016, 28 (33), 7185-7192; Energy Environ. Sci. 2012, 5, 9618; Nano Lett. 2015, 15, 3067; Appl. Phys. Lett. 105 (26), 263103]).

For this reason, we studied the variation of the work function of bare and of GO and $RGO_{-1.25V}$ coated SPE with macroscopic KP technique. The relevant results are depicted in Fig. S6 (black squares), where the work function of each samples is referred to the gold sample: $\Delta WF = WF - WF_{Au}$. For all modified samples, the measured WF is lower than the case of bare SPE corresponding to the effect of n-doping. The largest difference is achieved for $RGO_{-1.25V}$ modified SPE (*ca*. -400 meV). Similar values were obtained with KPFM (Fig. S6, red circles) by averaging the WF values measured on 10×10 μm^2 areas. Mean value and standard deviation values were calculated on 10 different areas on 2 samples for each modified SPE.

In general, both KP and KPFM are affected by the gradient of the total capacitance (C_T) between the tip and the sample which is described as the series of the quantum (C_q) and the bulk (C_B) capacitances: $\frac{1}{C_T} = \frac{1}{C_q} + \frac{1}{C_B}$. Tip-sample geometries of the two techniques are different, being 3 mm^2 parallel plates for KP [Bakie] and nanometric sphere (with a cone) on surface in the case of KPFM [Liscio Account]. In both geometries, the contribution of quantum capacitance can be ignored being much larger than the geometric tip-sample capacitance.

The excellent agreement between the WF values measured by the two techniques indicates that the contribution of quantum capacitance of $RGO_{-1.25V}$ and GO modified SPEs does not change, suggesting that C_q does not affect the change of the electrochemical property of the graphene-based

thin films on SPEs. We have to conclude that the different electrochemical behaviour of $RGO_{-1.25V}$ and GO in respect to $[Fe(CN)_6]^{3-/4-}$ redox system is due to a different conductivity of the bulk material.

3.4 Study of the electrocatalytic properties of GO and RGO

The evaluation of the electrocatalytic behaviour of GO and RGO films was then measured studying their ability to oxidize NADH and AA molecules in solution.

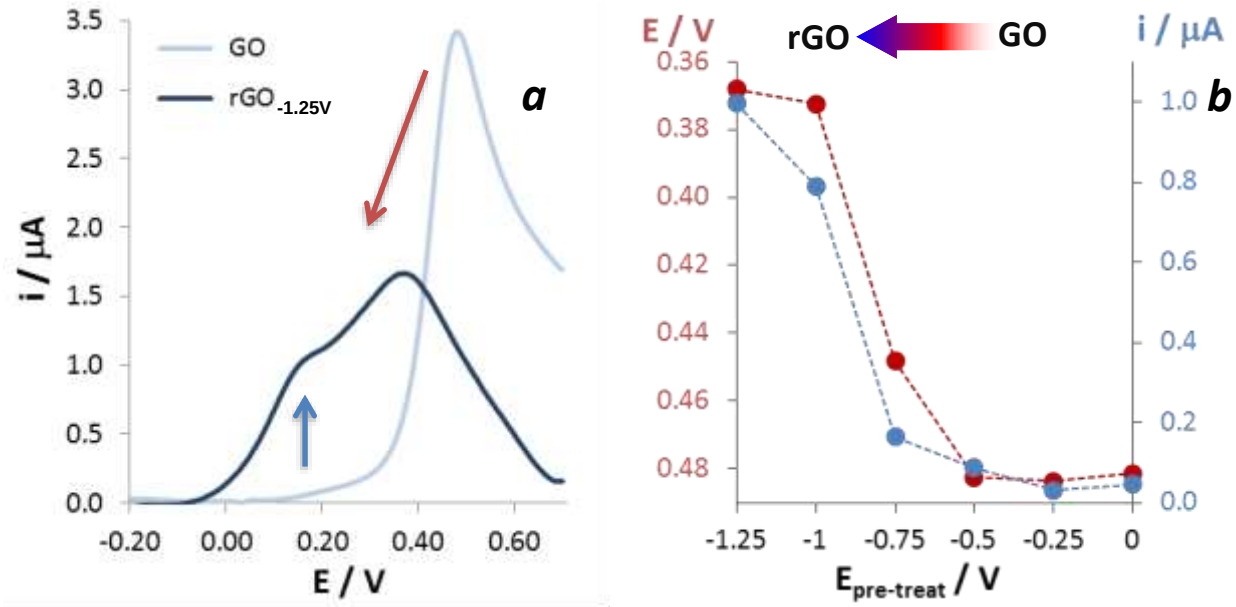

Fig. 5. *(a)* LSV traces obtained in 0.2 mM NADH, 0.1 M PBS (pH = 7.0) and 0.1 M KCl, at GO and $RGO_{-1.25V}$ modified SPEs (0.02 Vs^{-1} potential scan rate, background signal subtracted); *(b)* direct comparison of the shift of NADH oxidation peak potential (red arrow in *a*) and of the increase in current values measured at +0.17 V current peak (blue arrow in *a*) plotted versus the pre-treatment potential.

Voltammograms recorded in NADH solutions at GO and $RGO_{-1.25V}$ modified electrodes (Fig. 5*a*) show a significant shift of the oxidation peak from +0.47 V to +0.36 V. Furthermore, a new peak at ca. +0.17 V (blue arrow) is evident (the voltammograms of all the samples prepared are available in Fig. S7 in Supporting Information).

All RGO modified electrodes lead to record broader and lower peaks respect to pristine GO. This result can not be simply explained with the occurrence of electrocatalytic processes, which typically give a slight increase of the current peak [35, 38]. At difference to what proved from tests reported hereafter (see Paragraph *3.5*), the shape of the voltammogram in Fig. 5*a* more spontaneously suggests the occurrence of adsorption phenomena at $RGO_{-1.25V}$ surface. They may account for the lower height of the response with respect to that exhibited on GO. In particular, the oxidation at lower potentials

by passing from GO to RGO$_{-1.25}$ coatings could be explained assuming the occurrence of adsorption of products of the electrochemical process [40]. Such an adsorption step energetically favours the oxidation with respect to the diffusion-controlled process that is anyhow still contemporarily present [39].

Noteworthy, Fig. 5*b* shows that both the position of the original peak, shifting from +0.47 V to +0.36 V, and the current value of the new peak, arising at +0.17 V, follow the same trend observed for C/O ratio (Fig. 3*a*) as well for charge percolation and transfer resistance (Fig. 4*b*), previously reported. We can conclude that the behaviour of the material in respect to NADH oxidation is strictly related to the functional groups present on the electrode surface.

The most important effect of the electrochemical pre-treatment lies in the peak onset for the NADH oxidation, which decreases from +0.34 V to *ca.* +0.01 V by going from pristine GO to RGO$_{-1.25V}$/SPE. This constitutes the key advantage of the GO reduction to RGO, as to the electrochemical oxidation of such a species. It is well exploitable when considering the application of the material both in biosensing and in enzymatic biofuel cells.

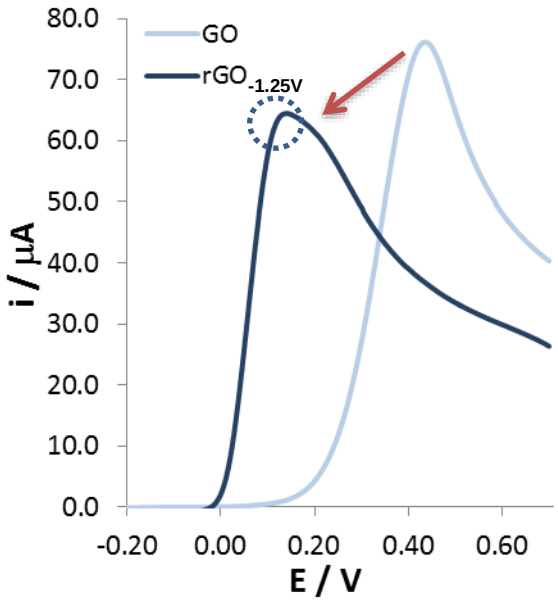

Fig. 6. LSV traces obtained in 4 mM AA, 0.1 M PBS (pH = 7.0) and 0.1 M KCl, at GO and RGO$_{-1.25V}$ modified SPEs (0.02 Vs^{-1} potential scan rate, background signal subtracted). Similar curves for all other samples are reported in Fig. S8 in Supporting Information.

The behaviour of RGO/SPEs is not specific of NADH oxidation: an even stronger peak anticipation (red arrow in Fig. 6) is observed in the oxidation of a different electroactive species, namely AA. The variation of the peak position by passing from untreated to electrochemically reduced graphene coatings once more follows the trend previously observed (data for all samples are available in Fig. S8 in Supporting Information): no significant change in RGO behaviour is observed for reduction potentials more positive than -0.75 V, whereas a significant peak anticipation is observed for electrochemical pre-treatment at potentials lower than -1.00 V. An oxidation peak at *ca.* +0.15 V is also evident (blue circle in Fig. 6) for $RGO_{-1.25V}$ modified SPE, even if in this case the two electrochemical responses are almost completely overlapped. Although the mechanism of AA oxidation is still a debated issue, it has been ascertained to involve adsorptions steps [41, 42], which could be the major cause of the results obtained here.

For both NADH and AA, the drastic change observed after pre-treatment at potential values as low as -0.75 V agrees well with the significant changes in the chemical composition of the surface observed by XPS (fig. 3*b*). It should be underlined that no variations of the voltammetric traces are observed for both NADH and AA oxidation by repeated cycling in the positive potential region; this indicates that the electrochemical pre-treatment at negative potential induces a stable modification of the surface chemistry of the material, which does not change during the sensing operations at positive potential.

3.5 *Functionalised graphite to mimic and explain RGO performance*

The results described above suggest to study the role played by residual C-OH, C=O and O-C=O functionalities on $RGO_{-1.25}$ nanosheets toward the oxidation of NADH and AA. Aiming at mimicking the chemical structure of graphene coatings, where oxygen functional groups are formed in correspondence to the break of the aromatic carbon structure, we chemically modified the surface of a bare SPE. As reported in the Experimental section, bare SPEs were electrochemically treated in sulphuric acid to increase the number of oxidized species (mostly carboxylic ones) on their graphite surface [25, 43]. The resulting SPE_{Act} was then further modified by depositing hydroquinone (HQ) and catechol (CT) onto, to increase the number of C-OH residues and, by electrochemical oxidation of these moieties, to create C=O groups on the surface [43, 44]. The occurrence of the actual anchoring of CT and HQ groups on the electrode surface is confirmed by the presence of quite a broad peak system detectable in the voltammetric curve recorded at HC/SPE, in PBS (Fig. S9 in the Supporting Information).

A significant anticipation of the current peak from +0.47 V to +0.36 V is observed for NADH, in the case of SPE_{Act}, with respect to bare SPE (Fig. 7*a*). The observed peak has shape and position

similar to one of the peaks recorded at $RGO_{-1.25}$ modified electrodes. Furthermore, the signal registered at HC/SPE surprisingly resembles that observed at $RGO_{-1.25}$/SPE: two well resolved anodic peaks are recorded in both cases. A similar result is obtained also for AA oxidation: the signal at HC/SPE closely resembles that registered at $RGO_{-1.25}$/SPE (Fig. 7*b*), although in this case the close proximity of the two peaks prevents from observing a significant variation in the shape of the voltammogram.

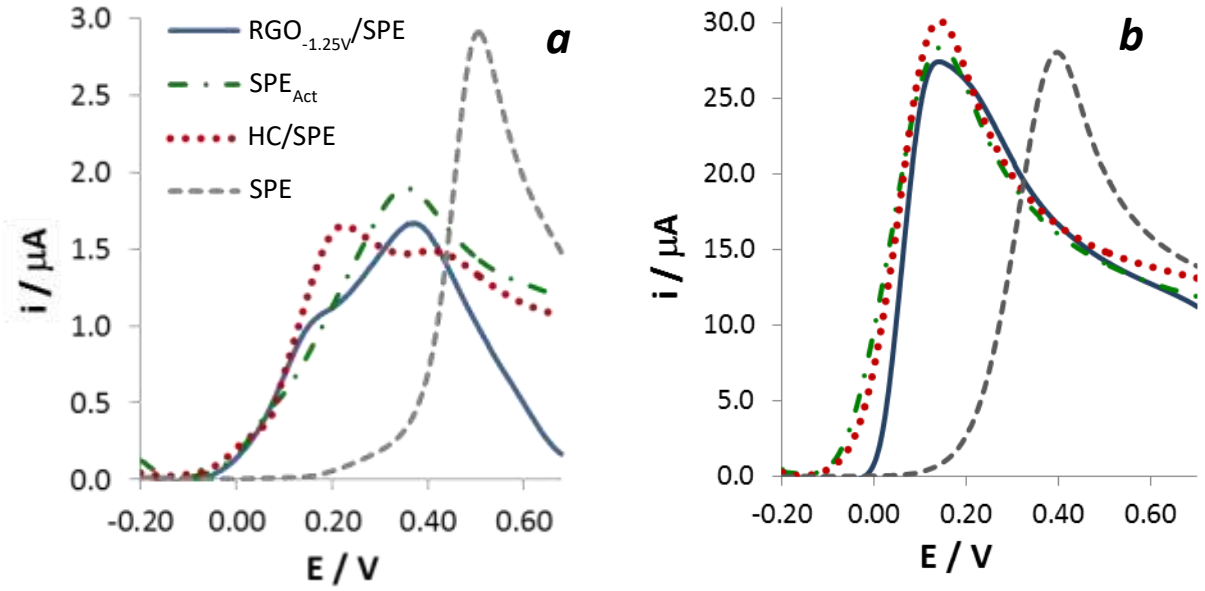

Fig. 7. Representative LSV traces for the RGO-coated SPE reduced at -1.25 V, the SPE activated by sulphuric acid, the SPE coated with HQ and CT and the pristine electrode, measured in two different solutions: *(a)* 0.2 mM NADH and (*b*) 4 mM AA, 0.1 M PBS (pH = 7.0) and 0.1 M KCl. Caption for *a* also holds for *b*. Background signal subtracted.

The above described electrochemical data strongly suggest that the good performance of RGO for NADH and AA oxidation is actually due to C-OH, C=O and O-C=O residues present on carbon-based surfaces. As observed from XPS spectrum of GO modified electrodes (Figs. 1*b* and 3*b*), these residues are already present on the pristine GO. However, they become electroactive only when the material becomes more conductive, thanks to the electrochemical pre-treatment (Fig. 4).

More specifically we can conclude that in the case of NADH oxidation, C-OH and C=O functional groups play a key role in the onset of a new oxidation peak at a low potential value. It should be underlined that HQ and CT derivatives are known to be efficient redox active mediators for NADH oxidation [20, 25, 45], but their practical use in electroanalysis is problematic due to their poor stability on the electrode surface. Conversely, the use of RGO provides a highly conductive, stable substrate, containing these residues.

3.6 Electrochemical performance of EGO

In the previous section we described the variations of physico-chemical properties of RGO films obtained by *in situ* electrochemical reduction: an improvement of the electrocatalytic performance of the material was demonstrated. However, the electrochemical pre-treatment constitutes an additional cost for the large scale production of a material. Graphite should be first oxidized to GO, then deposited on the electrodes, then partially reduced back to RGO. To avoid this complex procedure, we tested the electrocatalytic performance of a different graphene derivative, produced directly by electrochemical exfoliation of graphite, (EGO) [7, 16, 17, 26]. This approach allows us to obtain large quantities of graphene sheets in a very short time and in a single step, starting from bulk or powder graphite. It is much faster than the chemical production of GO by Hummer's methods, and yields larger sheets more soluble than those obtained typically by exfoliation of graphite in organic solvents by ultrasounds [46].

EGO was first characterized by XPS and Raman measurements (Fig. 8) in order to investigate the nature and amount of functional groups on the surface of this material. As to XPS, by considering both the C/O ratio and the height of different peaks of carbon-containing species we could observe that EGO has a chemical composition intermediate between $RGO_{-1.0}$ and $RGO_{-1.25}$. The Raman spectrum of EGO modified SPE (see Fig. 8b) was similar to those recorded for both GO and RGO samples, with well-defined D peak at 1350 cm^{-1} and G peak at 1596 cm^{-1}. It is worth noting that the I_D/I_G intensity ratio of EGO (1.18±0.01) is very close to the value of RGO (1.22±0.01), as shown in the inset of Fig.8*b*.

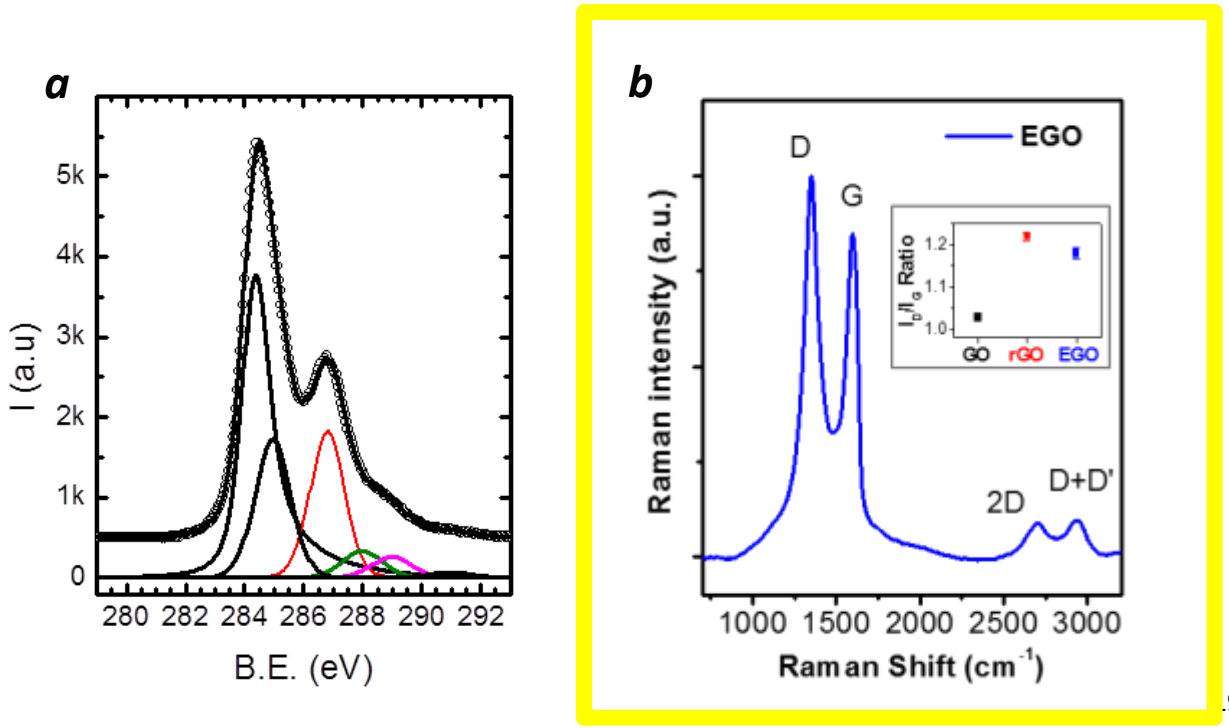

Fig. 8. *(a)* High resolution XPS and *(b)* Raman spectra of EGO/SPE; I_D/I_G peak intensity ratio of GO, $rGO_{-1.25V}$ and EGO modified SPEs is reported in the inset of *b*.

CV curves recorded on EGO/SPE in $[Fe(CN)_6]^{4-}$ aqueous solution are shown in Fig. 9. ΔE is similar to that measured at bare SPE and lower than that registered on GO coatings of similar thickness, indicating a lower resistance, of the EGO film respect to GO.

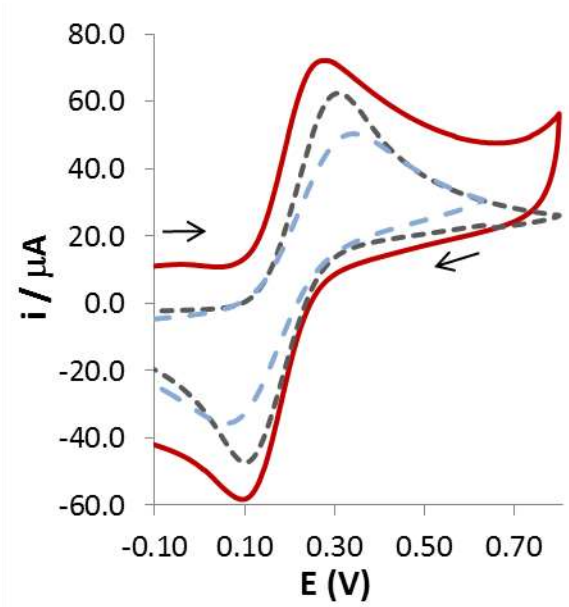

Fig. 9. Representative CV traces obtained in 5 mM $[Fe(CN)_6]^{4-}$, 0.1 M PBS (pH = 7.0) and 0.1 M KCl at EGO/SPE (red solid line), GO/SPE (light-blue dashed line) and bare SPE (dashed black line); 0.05 Vs^{-1} potential scan rate.

Similarly to what already discussed in the case of GO and RGO, the agreement between the WF values measured by KP and KPFM measurements (see Fig. S6 in the Supporting Information) indicates that C_q does not affect the effect of the electrochemical property of EGO films on SPEs as previously observed in the case of GO and RGO.

The electrocatalytic performance of EGO/SPE was compared with that of bare SPE and of GO/SPE, by using again the NADH anodic oxidation as the benchmark process (Fig. 10*a*). The results indicate that, without any electrochemical pre-treatment, the response is significantly anticipated also on EGO films with respect to bare electrodes: the relevant current peak shifts from +0.49 V to +0.37 V. Voltammetric traces also show a pre-peak in the +0.1 ÷ +0.2 V potential range (blue arrow in Fig. 10*a*), leading to significant anticipation of the peak onset. A similar result is also obtained for AA oxidation (Fig. 10*b*), demonstrating that the good performance of EGO is not specific for the

oxidation of a single chemical species, but is a more general feature of the material. This behaviour strongly resembles what already observed at RGO/SPEs (Figs. 5*a* and 6*a*) and, in consideration to surface functional groups evidenced by XPS measurements, may be ascribed to similar reasons.

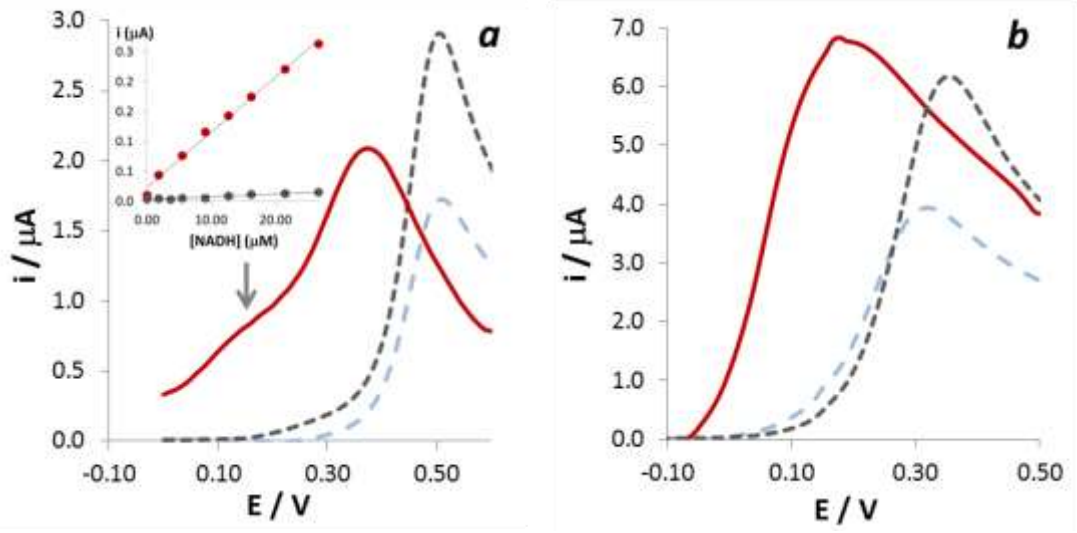

Fig. 10. LSV curves, subtracted for the relevant background, registered at EGO/SPE (red solid line), GO/SPE (light-blue dashed line) and bare SPE (dashed grey line) in *(a)* 0.2 mM NADH and *(b)* 0.4 mM AA, 0.1 M PBS (pH 7.0) and 0.1 M KCl; inset in *(a)* reports the calibration plots obtained from amperometric traces registered at +0.20 V under continuous stirring of the solution at EGO/SPE (red), and bare SPE (grey).

In order to demonstrate the actual possibility to oxidise NADH by measuring significant oxidation currents even at low potentials, chronoamperometric tests in presence and in absence of low concentrations of NADH (2 ÷ 30 µM) were performed at a very low potential (+0.20 V), using bare and EGO modified SPEs, respectively. This potential would normally be too low to detect NADH with commercial SPEs. Measurements performed on three bare and three EGO modified electrodes showed a strong difference between the sensitivity of the two electrode systems, confirmed by statistical t-test at a significance level of 95% (n=3). Amperometric tests, performed under continuous stirring of the solution, indicate that a linear dependence of the current values with respect to NADH concentration can be achieved at EGO/SPE, even at a fairly low potential value, namely +0.20 V (see inset of Fig. 10*a*). The sensitivity of EGO/SPE in this condition is more than fifteen times higher than that computed both on bare SPEs and on GO-coated SPEs, and lets us envision the application of EGO modified electrodes for NADH detection, even including the use in biosensors where NADH is produced by the enzymatic reaction, as well as in biofuel cell. The linear dependence of the oxidation current in respect to NADH concentration also demonstrates the good stability and

low passivation of EGO surface due to the electrochemical process, which is at the basis of the practical use of such a material in the previously cited applications.

4. Conclusions

The results described in this work indicate that GO constitutes a versatile material possessing tuneable conductivity and surface chemistry that make it suitable for applications in which the activation of electrocatalytic processes is required. The combination of spectroscopic and electrochemical analyses allowed us to correlate the physico-chemical properties of the material with the oxygen-based functional groups present on graphene nanosheets such as C-OH, C=O and O-C=O. Similar species are already present on pristine GO [13], but become active for the electrocatalytic process only when GO achieves a low electric resistivity.

Such low resistivity can be achieved with a pre-treatment of the electrode, consisting of an electrochemical reduction of GO/SPEs to RGO/SPEs that removes epoxide moieties and restores electrical conductivity while maintaining intact the chemical groups beneficial for NADH and AA oxidation.

A similar result can be also achieved in a single-step approach, using EGO. This material demonstrates very good electrocatalytic properties without the need of any electrochemical pre-treatment. It may be obtained in bulk scale directly by electrochemical oxidation of graphite, and used directly as a coating on commercial electrodes. The outstanding properties of this different graphene derivative let us envision the possible use of this material in the frame of amperometric sensors or of enzymatic biofuel cells.

The ascertained advantages of the use of RGO and EGO for NADH and AA anodic oxidation let us suppose that similar conclusions can be also achieved in electro-oxidation of species different from those specifically studied in the present article, further widening the application fields of these promising materials.

Acknowledgements

The research leading to these results has received funding from the European Union's Horizon 2020 research and innovation programme (grant agreement n°696656 Graphene Flagship) and the EC Marie-Curie ITN- iSwitch (GA no. 642196). Dr. Massimo Tonelli of the Centro Interdipartimentale Grandi Strumenti (CIGS - Università di Modena e Reggio Emilia) is acknowledged for the acquisition of the SEM images.

References

[1] Y. Shao, J. Wang, H. Wu, J. Liu, I.A. Aksay, Y. Lina, Graphene based electrochemical sensors and biosensors: a review, Electroanalysis 22 (2010) 1027-1036.

[2] S. Wu, Q. He, C. Tan, Y. Wang, H. Zhang, Graphene-based electrochemical sensors, Small 8 (2013) 1160-1172.

[3] M. Pumera, A. Ambrosi, A. Bonanni, E. L. K. Chng, H. L. Poh, Graphene for electrochemical sensing and biosensing, TrAC, Trends Anal. Chem. 29 (2010) 954-965.

[4] A. Ambrosi, C. K. Chua, A. Bonanni, M. Pumera, Electrochemistry of graphene and related materials, Chem. Rev. 114 (2014) 7150-7188.

[5] A. T. Lawal, Synthesis and utilisation of graphene for fabrication of electrochemical sensors, Talanta 131 (2015) 424-443.

[6] K.R. Paton, E. Varrla, C. Backes, R.J. Smith, U. Khan, A. O,ÄôNeill, et al. Scalable production of large quantities of defect-free few-layer graphene by shear exfoliation in liquids. Nat Mater 13 (2014) 624.

[7] Z.Y. Xia, S. Pezzini, E. Treossi, G. Giambastiani, F. Corticelli, V. Morandi, et al. The exfoliation of graphene in liquids by electrochemical, chemical, and sonication-assisted techniques: a nanoscale study, Adv. Funct. Mater. 23 (2013) 4684-4693.

[8] A. Liscio, G.P. Veronese, E. Treossi, F. Suriano, F. Rossella, V. Bellani, et al. Charge transport in graphene-polythiophene blends as studied by Kelvin Probe Force Microscopy and transistor characterization, J. Mater. Chem. 21 (2011) 2924-2931.

[9] C. Mattevi, G. Eda, S. Agnoli, S. Miller, K.–A. Mkhoyan, O. Celik, et al. Evolution of electrical, chemical, and structural properties of transparent and conducting chemically derived graphene thin films, Adv. Funct. Mater. 2009, 19, 2577-2583.

[10] F. Perrozzi, S. Prezioso, M. Donarelli, F. Bisti, P. De Marco, S. Santucci, et al. Use of optical contrast to estimate the degree of reduction of graphene oxide, J. Phys. Chem. C 117 (2013) 620-625.

[11] A. Ambrosi, M. Pumera, Precise tuning of surface composition and electron-transfer properties of graphene oxide films through electroreduction, Chem. Eur. J. 19 (2013) 4748-4753.

[12] C. S. Lim, A. Ambrosi, M. Pumera, Electrochemical tuning of oxygen-containing groups on graphene oxides: towards control of the performance for the analysis of biomarkers, Phys. Chem. Chem. Phys. 16 (2014) 12178-12182.

[13] K. H. Hui, A. Ambrosi, M. Pumera, A. Bonanni, Improving the analytical performance of graphene oxide towards the assessment of polyphenols, Chem. Eur. J. 22 (2016) 3830-3834.

[14] A. Vianelli, A. Candini, E. Treossi, V. Palermo, M. Affronte, Observation of different charge transport regimes and large magnetoresistance in graphene oxide layers, Carbon 89 (2015) 188-196.

[15] F. Perrozzi, S. Croce, E. Treossi, V. Palermo, S. Santucci, G. Fioravanti, et al. Reduction dependent wetting properties of graphene oxide, Carbon 77 (2014) 473-480.

[16] Z. Xia, F. Leonardi, M. Gobbi, Y. Liu, V. Bellani, A. Liscio, et al. Electrochemical functionalization of graphene at the nanoscale with self-assembling diazonium salts, ACS Nano 2016, 10, 7125-7134.

[17] Z. Y. Xia, D. Wei, E. Anitowska, V. Bellani, L. Ortolani, V. Morandi, et al. Electrochemically exfoliated graphene oxide/iron oxide composite foams for lithium storage, produced by simultaneous graphene reduction and $Fe(OH)_3$ condensation, Carbon, 84 (2015) 254-261.

[18] K. Parvez, Z.-S. Wu, R. Li, X. Liu, R. Graf, X. Feng, et al. Exfoliation of graphite into graphene in aqueous solutions of inorganic salts, J. Am. Chem. Soc. 136 (2014) 6083-6091. See also http://www.talgaresources.com/

[19] L. Wang, C. Kiang Chua, B. Khezri, R. D. Webster, M. Pumera, Remarkable electrochemical properties of electrochemically reduced graphene oxide towards oxygen reduction reaction are caused by residual metal-based impurities, Electrochem. Commun. 62 (2016) 17–20.

[20] A. Radoi, D. Compagnone, Recent advances in NADH electrochemical sensing design, Bioelectrochemistry 76 (2009) 126-134.

[21] A. Bello, M. Giannetto, G. Mori, R. Seeber, F. Terzi, C. Zanardi, Optimization of the DPV potential waveform for determination of ascorbic acid on PEDOT-modified electrodes. Sens. Act. B 121 (2007) 430-435

[22] M. Rasmussen, S. Abdellaoui, S. D. Minteer, Enzymatic biofuel cells: 30 years of critical advancements, Biosens. Bioel. 76 (2016) 91–102.

[23] S. Abdellaoui, R. D. Milton, T. Quah, S. D. Minteer, NAD-dependent dehydrogenase bioelectrocatalysis: the ability of a naphthoquinone redox polymer to regenerate NAD, Chem. Commun. 52 (2016) 1147-1150.

[24] F. Giroud, K. Sawada , Masahito Taya , S. Cosnier, 5,5-Dithiobis(2-nitrobenzoic acid) pyrene derivative-carbon nanotube electrodes for NADH electrooxidation and oriented immobilization of multicopper oxidases for the development of glucose/O_2 biofuel cells, Biosens. Bioel. 87 (2017) 957-963.

[25] C. Zanardi, E. Ferrari, L. Pigani, F. Arduini, R. Seeber, Development of an electrochemical sensor for NADH determination based on a caffeic acid redox mediator supported on carbon black, Chemosensors 3 (2015) 118-128.

[26] Z. Y. Xia, G. Giambastiani, C. Christodoulou, M. V. Nardi, N. Koch, E. Treossi, et al., Synergic exfoliation of graphene with organic molecules and inorganic ions for the electrochemical production of flexible electrodes, ChemPlusChem 79 (2014) 439-446.

[27] E. Treossi, M. Melucci, A. Liscio, M. Gazzano, P. Samorì, V. Palermo, High-contrast visualization of graphene oxide on dye-sensitized glass, quartz, and silicon by fluorescence quenching, J. Am. Chem. Soc. 131 (2009) 15576-15577.

[28] D. A. Dikin, S. Stankovich, E. J. Zimney , R. D. Piner, G. H. B. Dommett , G. Evmenenko et al., Preparation and characterization of graphene oxide paper, Nature 448 (2007) 457-460.

[29] S. Doniach, M. Sunjic, Many-electron singularity in X-ray photoemission and X-ray line spectra from metals, J Phys. C: Solid State Phys. 3 (1970) 285-291.

[30] S. Yumitori, Correlation of C_{1s} chemical state intensities with the O_{1s} intensity in the XPS analysis of anodically oxidized glass-like carbon samples, J. Mater. Sci. 35 (2000) 139-146.

[31] A. C. Ferrari, Raman spectroscopy of graphene and graphite: disorder, electron–phonon coupling, doping and nonadiabatic effects, Solid State Commun. 143 (2007) 47–57.

[32] S. Stankovich, R. S. Ruoff, R. D. Piner, K. A. Kohlhaas, A. Kleinhammes, Y. Jia et. al., Synthesis of graphene-based nanosheets via chemical reduction of exfoliated graphite oxide, Carbon 45 (2007) 1558-1565.

[33] G. K. Ramesha, S. Sampath, Electrochemical reduction of oriented graphene oxide films: an in situ raman spectroelectrochemical study, J. Phys. Chem. C 113 (2009) 7985-7989.

[34] A. J. Bard, L. R. Faulkner. Electrochemical methods. Fundamentals and applications. 2nd ed. New York: Wiley, New York; 2001.

[35] R. Seeber, L. Pigani, F. Terzi, C. Zanardi, Amperometric sensing. A melting pot for material, electrochemical, and analytical sciences, Electrochim. Acta 179 (2015) 350-363.

[36] D. Pletcher, R. Greff, R. Peat, L.M. Peter, J. Robinson. Instrumental methods in electrochemistry. Chichester: Horwood Publishing Ltd.; 2001.

[37] K. R. Ward , M. Gara, N. S. Lawrence, R. S. Hartshorne, R. G. Compton, Nanoparticle modified electrodes can show an apparent increase in electrode kinetics due solely to altered surface geometry: The effective electrochemical rate constant for non-flat and non-uniform electrode surfaces, J. Electroanal. Chem. 695 (2013) 1–9.

[38] R.S. Nicholson, Theory and application of cyclic voltammetry for measurement of electrode reaction kinetics, Anal. Chem. 37 (1965) 1351-1355.

[39] R. H. Wopschall, I. Shain, Effects of adsorption of electroactive species in stationary electrode polarography, Anal. Chem. 39 (1967) 1514-1527.

[40] A. Ambrosi, A. Bonanni, Z. Sofec, J. S. Cross, M. Pumera, Electrochemistry at chemically modified graphenes, Chem. Eur. J. 17 (2011) 10763-10770.

[41] G. Dryhurst, K. M. Kadish, F. Scheller, R. Renneberg, Ascorbic Acid. In: Biological electrochemistry, Vol.1, New York; Academic Press, Inc.; 1982, p. 256-278.

[42] M. Březina, J. Koryta, T. Loučka, D. Maršíková, J. Pradáč. Adsorption and kinetics of oxidation of ascorbic acid at platinum electrodes. J. Electroanal. Chem. 40 (1972) 13-17.

[43] R. L. McCreery, Carbon electrodes: structural effects on electron transfer kinetics. In: A. J. Bard, editor. Electroanalytical Chemistry, vol. 17, New York; Dekker; 1991 p. 221-374.

[44] T. Nagaoka, T. Yoshino, Surface properties of electrochemically pretreated glassy carbon, Anal. Chem. 58 (1986) 1037-1042.

[45] L. Gorton, E. Domínguez, Electrocatalytic oxidation of NAD(P)H at mediator-modified electrodes, Rev. Mol. Biotechnol. 82 (2002) 371-392.

[46] J. N. Coleman, Liquid exfoliation of defect-free graphene, Acc. Chem. Res. 46 (2013) 14-22.